



Role of organic admixtures on thaumasite precipitation

M.T. Blanco-Varela ^{a,*}, P.M. Carmona-Quiroga ^a, I.F. Sáez del Bosque ^a, S. Martínez-Ramírez ^{a,b}

^a Instituto de Ciencias de la Construcción Eduardo Torroja (IETcc-CSIC), C/Serrano Galvache 4, 28033 Madrid, Spain

^b Instituto de Estructura de la Materia (IEM-CSIC), C/ Serrano 121, 28006 Madrid, Spain

ARTICLE INFO

Article history:

Received 24 November 2011

Accepted 29 March 2012

Keywords:

Thaumasite

Cement (D)

Admixture (D)

Durability (C)

Temperature (A)

ABSTRACT

Thaumasite formation is normally a slow process; however some studies have shown that the presence of sucrose promotes its formation substantially. Many of today's concretes contain organic admixtures and no research has been conducted to date to determine whether the presence of these admixtures may induce or favour thaumasite formation. The present study aimed to ascertain whether, like sucrose, admixtures may further that process, and to propose a working methodology to do so.

The methodology used was: mixing sodium carbonate, sulfate and silicate solutions with a CaO solution with eleven commercial admixtures. The precipitates obtained after different curing times (up to 1 year) and temperatures (5 and 25 °C) were characterised with FTIR and XRD.

It was possible to distinguish between admixtures that did and those that did not favour thaumasite formation, i.e., products containing lignosulfonates or a mix of sodium carboxylate and polysulfonate as well as aluminium-based accelerating admixtures favoured thaumasite formation.

Published by Elsevier Ltd.

1. Introduction

Thaumasite is formed in concrete as a result of the reaction between sulfates and carbonates and the calcium silicate hydrates in the cement paste [1]. Statistical studies conducted in the UK have shown that sulfate attack and thaumasite formation are more prevalent in underground concrete exposed to low temperatures, high humidity, and environments with high sulfate contents, as well as concretes made with limestone aggregate [1]. Nonetheless, a number of cases of thaumasite-induced damage in concrete not exposed to those conditions have been reported [2–7]. Several studies have been reported showing that puzzolanic compounds, aluminium amount and even portlandite presence can reduce thaumasite formation [8–12].

Many of today's concretes contain organic admixtures (some comprising industrial by-products) that affect cement hydration in a variety of ways, modifying characteristics such as the dissolution or setting rates or paste flowability. Several recent reports have been published on thaumasite formation in gunned concrete in tunnels [13–15], where the concrete had been prepared using different superplasticisers and accelerating admixtures to improve the workability of the fresh material and its adherence to tunnel walls and crown.

To date, science has not addressed the question of whether the presence of these admixtures may induce or favour thaumasite formation and whether that might explain damage observed in concrete in temperate or warm climates [2,5], young concrete or mortar not exposed to high sulfate ion concentrations [16].

Thaumasite formation is usually, although not always, a slow process [4], whose reaction kinetics are governed by the slowest stage, the expansion of the tetrahedral Si coordination sphere in the C–S–H gel to the octahedral configuration in thaumasite [17,18].

Studies on thaumasite synthesis have shown that the presence of sucrose promotes its formation substantially [19–21]. Although the role of sucrose in the expansion of the Si coordination sphere is still under study, this compound is known to form an adduct with the Ca²⁺ ions in the solution, increasing portlandite solubility [21]. Moreover, Kinrade et al. [22] showed that certain aliphatic polyhydric alcohols readily yield solutions containing high concentrations of stable silicate anions in which the silicon may be penta- or hexa-coordinated with oxygen. To be able to generate significant amounts of such complexes, the polyalcohol must have at least four adjacent hydroxy groups, two with a threo configuration.

Thaumasite formation is normally a slow process; however some studies have shown that the presence of sucrose promotes its formation substantially, then the present study aimed to ascertain whether, like sucrose, admixtures may further thaumasite formation.

To this end, the methodology used was the same as for thaumasite synthesis [20]: i.e., mixing sucrose solutions of carbonate, sulfate and sodium silicate with a CaO sucrose solution, but replacing the sucrose solution with one of two concentrations of commercial admixtures solution.

2. Experimental

For all the eleven admixtures, 2 different proportions of each particular admixture (Table 2) were used to prepare a series of calcium

* Corresponding author. Tel.: +34 913020440; fax: +34 913026047.

E-mail address: blancomt@ietcc.csic.es (M.T. Blanco-Varela).

oxide, admixture and water mixes (mix X in Table 1). A series of aqueous solutions of sodium carbonate, sulfate and silicate were also prepared, with compositions as given in Table 1 (mix Y). After preparation and chilling to 5 °C or keeping at 25 °C, Y was poured over X and the mixes were stirred for 5 min in a closed container at 5 or 25 °C. After 1, 2, 3, 6 or 9 months or 1 year (or even up to 3 years) samples were filtered and obtained precipitated solid were examined by XRD and FTIR techniques. A reference aqueous mix containing the same oxide compositions as in Table 1 but no admixtures, was prepared and kept at 5 °C for 1 year. After this time the sample was filtered and analysed by FTIR.

Table 2 gives the name and amount of admixture added to the X mix. The proportion of admixture added to the solution was determined on the grounds of manufacturer recommended maximum and minimum amounts per kg of cement and assuming a water/cement ratio of 1/2.

FTIR spectra were obtained on a Thermo Scientific Nicolet 600 spectrometer. Samples were prepared by mixing 1 mg of sample in 300 mg of KBr. Spectral analysis was performed over the range 4000–400 cm^{−1} at a resolution of 4 cm^{−1}.

A Bruker D8 Advance X-ray diffractometer consisting of a high voltage, 3-kW generator and a (1.54-Å CuKα) copper anode X-ray tube normally operating at 40 kV and 50 mA, was used for the mineralogical characterisation of the samples. This instrument was coupled to a Lynxeye detector with a 3-mm anti-scatter slit and a (0.5%) Ni K-beta filter, with no monochromator. Patterns were recorded over the angular range 5–60° 2θ, with a step size of 0.02° 2θ, and a cont time of 5 s per step.

Thermodynamic modelling was carried out using the Gibbs free energy minimization program GEMS [23], with the internally consistent thermodynamic data set [24] expanded with the cement-specific database (CEM DATA) compiled in Ref. [25].

3. Results

Tables 3 and 4 summarise the crystalline phases identified by XRD in the precipitates obtained at 25 and 5 °C, respectively, at ages of up to 1 year.

At the concentrations and temperatures studied, portlandite and calcite were the only two crystalline phases detected at any age on the XRD traces for the precipitates from the solutions containing polycarboxylate- (superplasticisers, samples 6, 7, 8 and 11) or thiocyanate-based (accelerating admixture, sample 4) admixtures. The much lower intensity and greater width of the calcite than the portlandite diffraction lines denoted the lower proportion and poorer crystallisation of the former. No crystalline sulfate or tobermorite-type C–S–H gel was detected (Fig. 1 shows the XRD patterns of two of these samples, 7 and 8). The XRD traces for samples 5A and 5B (nitrate-based admixture) stored at 25 °C for up to 1 year yielded similar findings (XRD patterns not shown).

The FTIR spectra for the 3-month samples (Fig. 2), contained bands generated by the O–H bond stretching vibrations in portlandite (3643 cm^{−1}) and water (3435 cm^{−1}); a medium intensity band at around 1641 cm^{−1} attributable to the H–O–H bending vibrations in water; and a wide, intense band from 1400 to 1500 cm^{−1} due to the asymmetrical C–O bond stretching vibrations in carbonate groups,

Table 1
Concentration of solutions X and Y.

	X		Y	
Reagent	CaO	Na ₂ SiO ₃	Na ₂ SO ₄	Na ₂ CO ₃
Mass	5.05 g	1.83 g	7.1 g	1.59 g
Volume/solvent	250 ml/water + xg admixture		250 ml/water	
Concentration X + Y	0.18 M	0.03 M	0.1 M	0.03 M
Volume X + Y	500 ml			

Table 2
Admixture type, chemical base and concentration.

Admixture type	Chemical base	Name	g admixture/ 0.5 l solvent	Name	g admixture/ 0.5 l solvent
Superplasticiser	Lignosulfonate	1A	6	1B	3
Accelerating	KAl(OH) ₄	2A	6	2B	3
Accelerating	Al ₂ (SO ₄) ₃ ·14H ₂ O	3A	6	3B	3
Accelerating	Thiocyanate	4A	2	4B	0.5
Accelerating	Nitrate	5A	2	5B	1
Superplasticiser	Polycarboxylate	6A	1	6B	0.3
Superplasticiser	Polycarboxylate	7A	0.3	7B	0.1
Superplasticiser	Polycarboxylate	8A	0.3	8B	0.1
Plasticiser	Lignosulfonate	9A	6	9B	3
Retarding	Sodium carboxylate + polysulfonate	10A	15	10B	5
Superplasticiser	Polycarboxylate	11A	14	11B	5

whose ν₂ and ν₄ vibrations were observed at 872 and 712 cm^{−1}, respectively, and attributed to the poorly crystallised calcite detected by XRD. The medium and small bands in the 1100–1130 cm^{−1} area and at around 671 cm^{−1} were respectively interpreted to reflect sulfate group S–O bond symmetrical and bending vibrations. This sulfate might be amorphous or its proportion must have been below the XRD detection limit, since they were not observed on the diffractogram but were detected by FTIR. Lastly, the wide, medium intensity band at 900–1000 cm^{−1} and the weaker band at around 815 cm^{−1} were interpreted to be due to asymmetrical stretching vibrations generated by the Si–O bond in the C–S–H gel. These spectra were similar to the 1-year spectra for the same samples.

XRD data show (Figs. 3 and 4) that regardless of the admixture concentration, temperature and curing age, all solid precipitates obtained from mixes containing aluminium comprised of ettringite, calcite as well as, gypsum, brucite and portlandite, at some ages. The broad peak 2θ = 9.0–9.3° detected in the XRD patterns of the precipitates obtained from samples 3A and 3B at 5 and 25 °C after already 3 months of reaction can be attributed to the formation of thaumasite and/or ettringite–thaumasite solid solution. After Barnett et al. studies [26], the solid solution effect on structure can be observed by XRD, since the positions of the peaks due to each phase are changing.

It was noticed that while ettringite peak was decreasing, thaumasite peak was rising over the time (Fig. 3) and after one year, reflexions of both phases could be distinguished. The amount of thaumasite was higher in the chill-cured samples with a lower proportion of admixture (3B at 5 °C). The precipitates obtained from the admixture 2, in turn, only contained thaumasite when cured at 5 °C with the smaller amount of admixture (2B) (Fig. 4).

FTIR spectra of the 3-month samples which were in contact with admixture 3 (Fig. 5) showed bands characteristic of ettringite, calcite; brucite (OH stretching at 3680 cm^{−1}); and possibly portlandite, since the OH stretching vibrations in this phase may overlap with the ettringite vibrations.

After only 90 days (Fig. 5), the spectra exhibited bands characteristic of the octahedral silicon in thaumasite (SiO₆ stretching and bending, 500 and 760 cm^{−1}) in samples 3A and 3B stored at 5 and 25 °C indicating thaumasite and/or solid solution ettringite–thaumasite formation. Furthermore, the low intensity of the absorption bands in the (tetrahedral silicon) C–S–H gel Si–O stretching vibration area (1000–900 cm^{−1}) was an indication that practically no gel was formed, i.e., that this admixture inhibited C–S–H precipitation. Over time, these chill-cured samples evolved towards thaumasite formation (3500, 3470, 3400, 1700; 1655; 1400; 1100; 871; 760; 676; 646; 587; and 500 cm^{−1}).

After 1 year (Fig. 6) the carbonates clearly shifted to 1400 cm^{−1}, and whereas the bands due to tetrahedrally coordinated silicon Si–O vibrations (1000–900 cm^{−1}) disappeared altogether, bands associated with ettringite were still visible, denoting its presence in the sample.

Table 3

Crystalline phases identified by XRD in the precipitates obtained at 25 °C and at different ages by using two proportions (A and B) each of the eleven admixtures.

A	3 months	6 months	9 months	1 year	B	3 months	6 months	9 months	1 year
1	P,c,+	–	–	P,c,t,+ ^a	1	P,c,+	–	–	P,c,+ ^a
2	E,c,g	^a	E,c,g,AFm	^a	2	E,c,p	^a	^a	^a
3	E,t,c,p,b	^a	^a	E,t,c	3	E,t,c,p,b	^a	E,T,c,p,b	^a
4	P,c	^a	^a	–	4	–	–	–	–
5	P,c	^a	^a	C,p	5	P,c	^a	^a	P,c,e
6	P,c	^a	^a	–	6	P,c	^a	^a	–
7	P,c	^a	^a	–	7	P,c	^a	^a	–
8	P,c	^a	^a	–	8	P,c	^a	^a	–
9	P,c	–	–	P,c,+	9	P,c	–	–	P,c,+
10	P,c,+	–	–	+ ,p,c	10	P,c	–	–	P,c,+
11	P,c	–	–	P,c	11	P,c	–	–	–

p = portlandite; e = ettringite; c = calcite; t = thaumasite; AFm = calcium monosulfaluminate hydrate; b = brucite; g = gypsum; e-tss = ettringite–thaumasite solid solution; capital letters = main phase; + = weddellite.

^a = no changes in the phases present were noted compared to the relevant earlier sample.

Table 4

Crystalline phases identified by XRD in the precipitates obtained at 5 °C and at different ages by using two proportions (A and B) each of the eleven admixtures.

A	1 months	2 months	3 months	6 months	9 months	1 year	B	1 months	3 months	6 months	9 months	1 year
1	–	P,t,c	^a	–	–	T,p,c,+	1	P	P,t,c	–	–	P,t,c,+ ^a
2	–	–	E,c	^a	C,e,g	E,c	2	–	E,c,t,p	^a	^a	^a
3	–	–	E-Tss, c,p,b	^a	^a	^a	3	–	T,E,c,p,b	^a	^a	^a
4	–	–	P,c	^a	^a	–	4	–	P,c	^a	^a	–
5	–	–	P,c	P,t,c	^a	^a	5	–	P,c	P,c,t	^a	^a
6	–	–	P,c	^a	^a	–	6	–	P,c	^a	^a	–
7	–	–	P,c	^a	^a	–	7	–	P,c	^a	^a	–
8	–	–	P,c	^a	^a	–	8	–	P,c	^a	^a	–
9	P	P,t,c	^a	–	–	P,t,c,+	9	–	P,c	–	–	P,c,t,+
10	P,c	P,c,+	^a	–	–	P,c,+	10	P	P,c	–	–	P,c,t,+
11	P	^a	P,c	–	–	P,c	11	–	P,c	–	–	–

p = portlandite; e = ettringite; c = calcite; t = thaumasite; b = brucite; g = gypsum; e-tss = ettringite–thaumasite solid solution; capital letters = main phase; + = weddellite.

^a = no changes in the phases present were noted compared to the relevant earlier sample.

The spectra for the 3A and 3B samples cured at 5 °C varied similarly over time, although the thaumasite bands were consistently more intense in the samples with lower concentrations of admixture (Fig. 6).

FTIR spectra of samples which were in contact with admixture 2 (aluminium and potassium hydroxide-based accelerating admixture for gunned concrete, Fig. 7), at all ages shown bands associated with ettringite (3644, 1110 and 610 cm^{−1}) and calcite (1430; 875 and 712 cm^{−1}) Portlandite and thaumasite bands were also observed on the spectra for the samples stored at 5 °C containing the lower concentration of the admixture (2B). The band attributed to ν₃ Si–O

bond vibrations in the C–S–H gel (around 960 cm^{−1}), exhibited relatively low intensity at all ages and disappeared at the expense of thaumasite formation.

When the admixture concentration was lower at 5 °C, the XRD traces for the 1-month precipitates obtained in the presence of a lignosulfonate-based admixture (samples 1 and 9, superplasticiser and plasticiser, respectively) contained only portlandite reflections (Table 4 and Fig. 8), although the wider and increasingly more

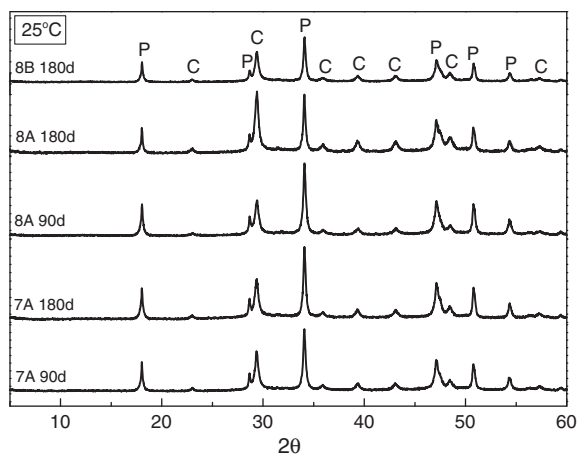


Fig. 1. XRD patterns of precipitates obtained from solutions containing polycarboxylate admixtures (7A, 8A and 8B) at 25 °C and at different ages (90 and 180 days). P = portlandite; C = calcite.

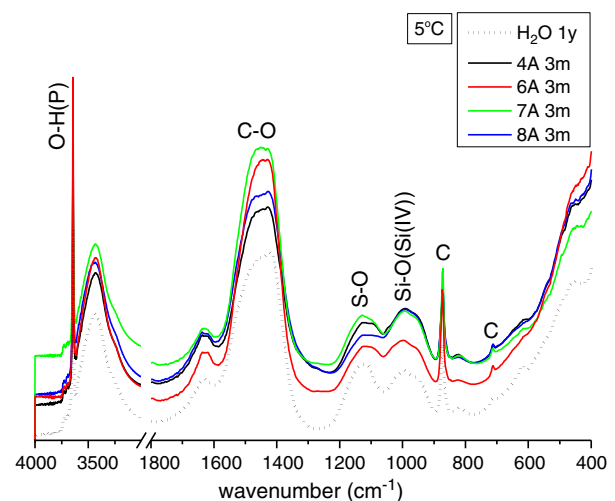


Fig. 2. FTIR spectra of precipitates obtained from solutions containing polycarboxylate (6A, 7A, 8A) or thiocyanate (4A) admixtures at 5 °C for 3 months and of precipitate in water (without admixtures) after 1 year is shown as reference. P = portlandite; S–O = sulfate vibration; Si–O(Si(IV)) = tetrahedral silicate vibration from C–S–H gel.

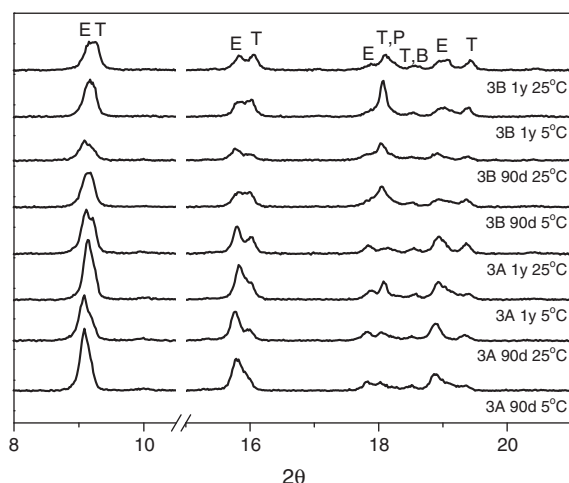


Fig. 3. Detail of XRD patterns of precipitates obtained from solutions containing aluminium sulfate hydrate as admixture (3A and 3B) at different ages (90 days and 1 year) and temperatures (5 and 25 °C). P = portlandite; E = ettringite; T = thaumasite; B = brucite.

intense reflections that appeared over time were assigned to poorly crystallised calcite. After 2 or 3 months, the diffractograms for the precipitates stored at 5 °C also contained small thaumasite reflections whose intensity increased with time, but which did not appear at such early ages for the samples stored at 25 °C. Nonetheless, the 1-year pattern for the sample 1A precipitate cured at 25 °C contained intense diffraction lines attributable to thaumasite (Fig. 8). For the samples at later ages weddellite was also observed.

The FTIR spectra for the 1-month to 1-year samples stored at 5 °C (Fig. 9) confirmed the XRD findings. The 1-month samples generated wide bands in the carbonate and sulfonate group vibration areas, which may be an indication of their amorphous nature. An intense, narrow band was also observed in the O–H group stretching vibration area, denoting the presence of portlandite. The bands in the Si–O ν_3 vibration area associated with the C–S–H gel (at around 950 cm^{-1}) were also wide but scanty intense and very likely overlapped with some of the admixture bands (1045 cm^{-1}).

A comparison of the FTIR spectra for the 1-month and 1-year samples (Fig. 9) revealed a shift in the carbonate C–O asymmetrical stretching bands to lower frequency numbers, centred at around 1400 cm^{-1} ; higher intensity of the sulfate S–O asymmetrical stretching band, centred at around 1100 cm^{-1} ; a decline in the Si–O asymmetrical stretching band associated with tetrahedrally coordinated silicates; and

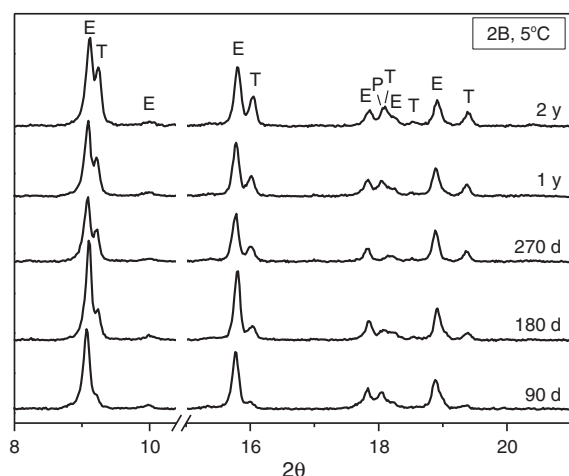


Fig. 4. Detail of XRD patterns of precipitates obtained from solutions containing potassium aluminium hydroxide as admixture (2B) at 5 °C and at different ages (90, 180, 270 days, 1 year and 2 years). P = portlandite; E = ettringite; T = thaumasite.

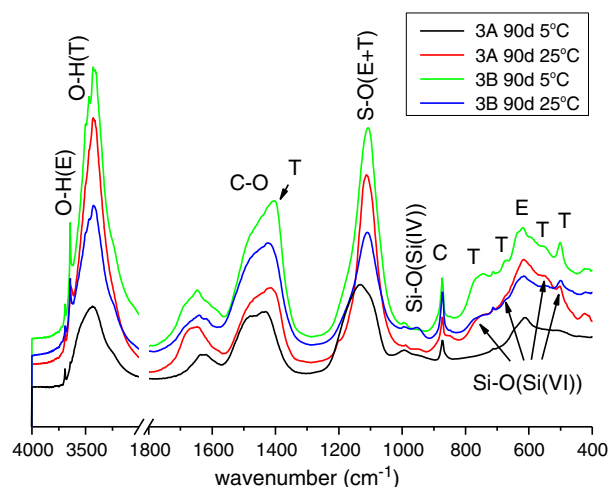


Fig. 5. FTIR spectra of precipitates obtained from solutions containing aluminium sulfate hydrate as admixture (3A and 3B) at 90 days and at different temperatures (25 and 5 °C). P = portlandite; E = ettringite; T = thaumasite; C = calcite; C–O = carbonates; S–O = sulfate vibration; Si–O(Si(IV)) = tetrahedral silicate vibration from C–S–H gel; Si–O(Si(VI)) = octahedral silicate vibration from thaumasite.

the appearance of SiO_6 (octahedral silicon) bands. All these observations are indicative of the presence of thaumasite.

The diffractograms for the 180-day precipitates obtained with a nitrate-based product (accelerating admixture, samples 5A and 5B) stored at 5 °C (Fig. 10) contained a low intensity diffraction line at $2\theta = 9.25^\circ$, in addition to the calcite and portlandite reflections. The intensity of this third reflection grew with time and was clearly attributable to thaumasite in the samples stored at the low temperature for 270 and 365 days (Fig. 10).

The FTIR spectra for these samples (5A as an example in Fig. 11) showed a clear change after 90 days. The OH group vibrations present in thaumasite appeared as a signal in the 3650–3400 cm^{-1} area. The absorption associated with tetrahedral Si–O ν_3 vibrations declined, while the Si–O bands denoting the presence of octahedrally coordinated silicon characteristic of thaumasite became gradually more intense. The ν_3 vibration bands for the C–O groups, in turn, were observed to shift from 1435 cm^{-1} at the earlier ages to 1400 cm^{-1} (denoting the thaumasite carbonates) by the end of the trial (up to 3 years in this case). At the same time, the S–O ν_3 bands grew narrower and shifted to 1100 cm^{-1} ,

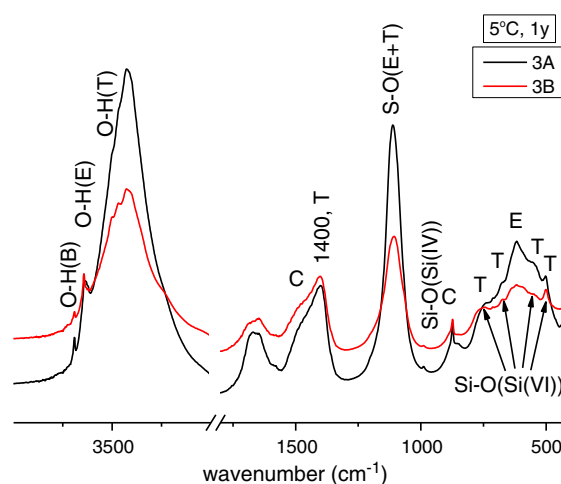


Fig. 6. FTIR spectra of precipitates obtained from solutions containing aluminium sulfate hydrate as admixture (3A and 3B) after 1 year at 5 °C. P = portlandite; E = ettringite; T = thaumasite; C = calcite; B = brucite; S–O = sulfate vibration; Si–O(Si(IV)) = tetrahedral silicate vibration from C–S–H gel; Si–O(Si(VI)) = octahedral silicate vibration from thaumasite.

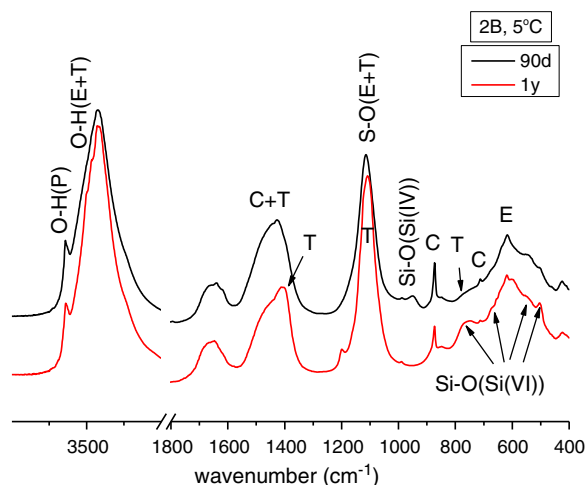


Fig. 7. FTIR spectra of precipitates obtained from solutions containing potassium aluminium hydroxide as admixture (2B) after 90 days and 1 year at 5 °C. P = portlandite; E = ettringite; T = thaumasite; C = calcite; S-O = sulfate vibration; Si-O(Si(IV)) = tetrahedral silicate vibration from C-S-H gel; Si-O(Si(VI)) = octahedral silicate vibration from thaumasite.

indicating a change in these groups toward the sulfate environment in thaumasite.

Finally, portlandite, calcite and weddellite were the sole crystalline phases detected on the diffractograms for the precipitates obtained in the sodium carboxylate + polysulfonate-type product (retarding admixture, samples 10A and 10B) (Tables 3 and 4) with one exception: sample 10B stored at 5 °C also contained lines indicative of thaumasite (Fig. 10).

The FTIR spectra for the 10A samples (not shown) contained intense bands attributable to portlandite, sulfates and carbonates, and only weak bands in the ν_3 Si-O vibration area. A decrease of the admixture concentration (10B sample), favoured the calcium silicate hydrate precipitation and inhibited calcium sulphate formation at early ages, (Fig. 12). FTIR spectrum of sample 10B preserved at 5 °C for 1 year presents bands clearly attributable to thaumasite whereas the band ν_3 Si-O (Si(IV)) towards 990 cm^{-1} has almost disappeared.

4. Discussion

The methodology used in the study was based on a procedure described by Strübe to synthesise thaumasite [19], and modified by Aguilera et al. [20]. The CaO and sodium salt concentrations used in this study were as described in prior articles [20,21], replacing the

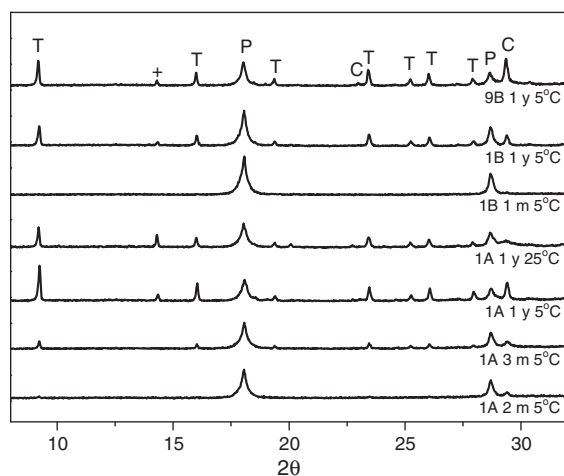


Fig. 8. Detail of XRD patterns of precipitates obtained from solutions containing lignosulfonates as admixture (1A, 1B and 9B) at 5 °C (1A also at 25 °C) and at different ages (1 month, 2, 3 months and 1 year). P = portlandite; C = calcite; T = thaumasite; + weddellite.

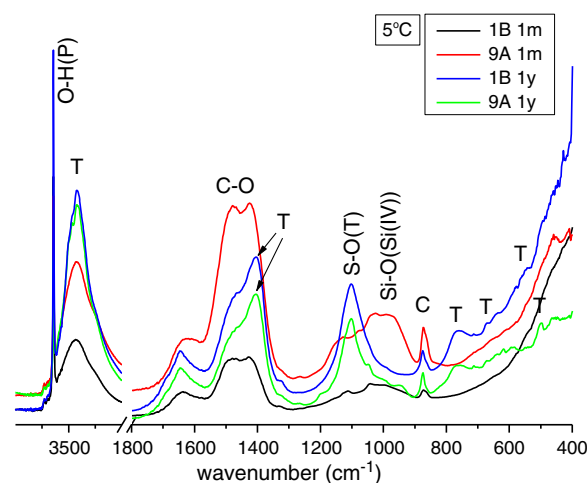


Fig. 9. FTIR spectra of precipitates obtained from solutions containing lignosulfonates as admixtures (1B and 9A) kept at 5 °C at different ages (1 month and 1 year). P = portlandite; C = calcite; T = thaumasite; C-O = carbonates; S-O = sulfate vibration; Si-O(Si(IV)) = tetrahedral silicate vibration from C-S-H gel.

sucrose with admixtures at concentrations in keeping with the minima and maxima recommended in their respective data sheets.

Thermodynamic modelling of the mix containing solutions X + Y in water (without admixtures) at 5 and 25 °C in a closed system predicts the precipitation of thaumasite and portlandite. In the absence of admixtures which serve as a “catalysts”, the reaction rate was very slow and phases present in precipitates were identified at both temperatures as calcite, C-S-H gel and portlandite in agreement with experimental data where no gypsum was identified. The equilibrium composition of the solutions with those phases shows the values given in Table 5.

In the present study, whenever polycarboxylate-type superplasticisers or thiocyanate accelerating admixtures (samples 6, 7, 8, 11 and 4) were added to the mix, portlandite precipitated as the major crystalline phase, along with a much smaller quantity of calcite. The FTIR spectra, however, exhibited bands that denoted the presence of C-S-H gel and sulfates (amorphous or absorbed on C-S-H [27,28]) in the precipitates as well. The similarity of these bands to the signals detected for the admixture-free control precipitate (Fig. 2) indicated that the admixtures neither inhibited C-S-H gel precipitation nor apparently affected the normal precipitation of the phases obtained during cement hydration. According to Neville [29], superplasticisers

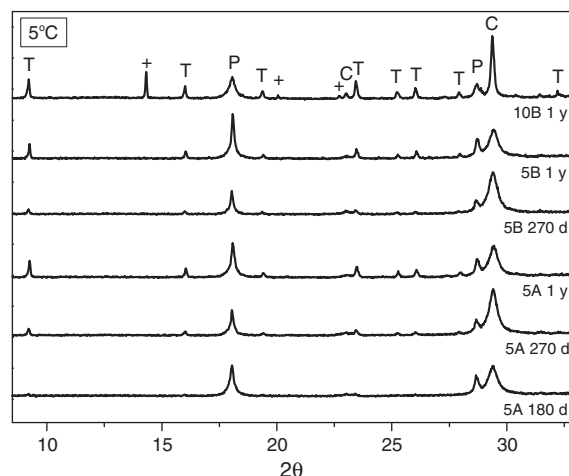


Fig. 10. Detail of XRD patterns of precipitates obtained from solutions containing an admixture based on nitrate (5A or 5B) and a mix of lignosulfonate and sodium carboxylate (10B) at 5 °C and at different ages (180, 270 days and 1 year). P = portlandite; C = calcite; T = thaumasite; + weddellite.

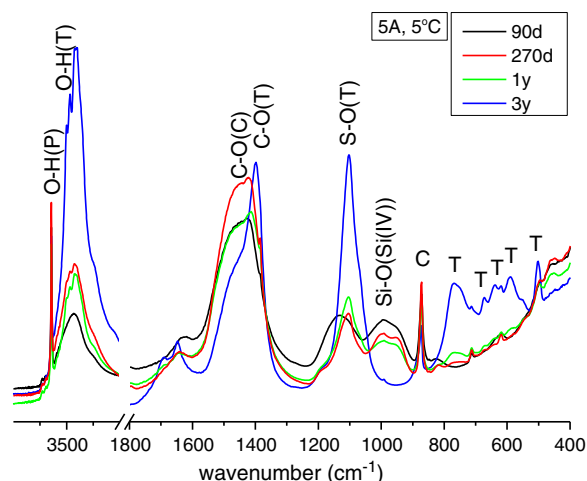


Fig. 11. FTIR spectra of precipitates obtained from solutions containing an admixture based on nitrate (5A) at 5 °C and at different ages P = portlandite; C = calcite; T = thaumasite; C-O = carbonate vibration; S-O = sulfate vibration; Si-O(Si(IV)) = tetrahedral silicate vibration from C-S-H gel.

do not alter the structure of hydrated cement paste in any fundamental manner. The main effect is a more uniform distribution of cement particles, with the formation of ettringite crystals which are small and nearly cubic in shape rather than needle-like.

The low intensity of the bands at around 900–1000 cm⁻¹ on the spectra for samples 2 and 3 signified that the precipitation of C-S-H gel was perceptibly inhibited from the earliest ages when the admixture used was an aluminium salt. This may have been due to a decrease in the Ca concentration in the solution as a result of the precipitation of ettringite, the majority crystalline phase in these samples.

When aluminium sulfate (sample 3) was used as the admixture, the Si-O vibration bands characteristic for octahedrally coordinated silicon appeared at the earliest age analysed (90 days), denoting either the early precipitation of thaumasite or the initial presence of an ettringite–thaumasite solid solution. With time, the thaumasite content increased in these precipitates at the expense of ettringite and after 1 year thaumasite was the majority crystalline phase.

The rate of thaumasite formation and its content in the precipitate was higher when the admixture contained aluminium sulfate than when

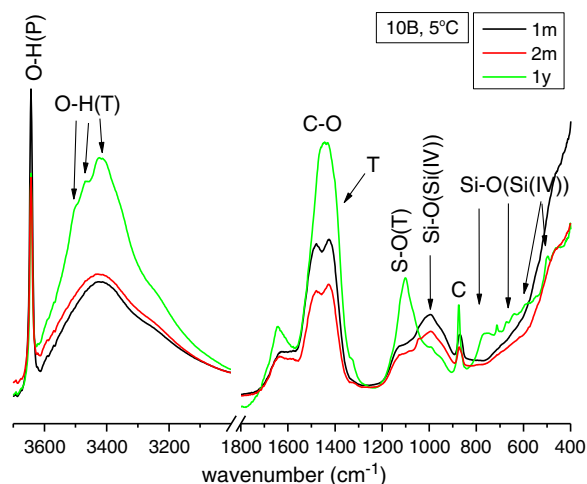


Fig. 12. FTIR spectra of precipitates obtained from solutions containing an admixture based on a mix of lignosulfonate and carboxylate (10B) at 5 °C and at different ages (1 month, 2 months and 1 year). P = portlandite; C = calcite; T = thaumasite; C-O = carbonate vibration; S-O = sulfate vibration; Si-O(Si(IV)) = tetrahedral silicate vibration from C-S-H gel; Si-O(Si(VI)) = octahedral silicate vibration from thaumasite.

Table 5

Initial composition of the mixture solution (mol/l) and predicted final solution compositions in equilibrium with calcite, C-S-H gel and portlandite at 5 and 25 °C (mmol/kg).

	M (initial)	mmol/kg (5 °C)	mmol/kg (25 °C)
C	0.03	0.0594	0.0467
Ca	0.18	9.933593	7.8949055
Na	0.32	320.16187	320.16217
S	0.1	100.04662	100.04671
Si	0.03	0.0463	0.0386
pH		13.70	12.95

it contained sodium aluminate, most likely due to greater concentration of sulphate ions in the solution. Aluminium has been reported to accelerate thaumasite formation [16,30] and some authors [26,31,32] detected the existence of an Ett-Th solid solution in which a small amount of Al is replaced by Si in the ettringite structure.

When lignosulfonate was used as an admixture (samples 1 and 9, superplasticiser and plasticiser for gunned concrete, respectively), the precipitate initially contained portlandite, amorphous CaCO₃ [33] (later crystallizing to the calcite identified by XRD at later ages), likewise amorphous sulfates and amorphous calcium silicates. In the samples stored at 5 °C, thaumasite was identified after just 2 months and its content was observed to grow throughout the trial. After 1 year, thaumasite was identified in only one of the samples cured at 25 °C, 1A, but not in 1B, 9A or 9B.

Lignosulfonate admixtures favoured the expansion of the Si sphere of coordination and thaumasite precipitation, but without wholly inhibiting the precipitation of calcium silicates. While nothing in the literature confirms that lignosulfonates furthers the octahedral coordination of Si, commercial lignosulfonate-based admixtures often contain lower amounts of sugar which, as noted earlier, forms a complex with Ca²⁺. The presence of weddellite in some of these samples could be an indication of presence of carbohydrates in the lignosulfonate admixtures, taking into account that oxalic acid has been reported as a product of carbohydrates oxidation reaction [34] and weddellite has been identified in synthesis of thaumasite in sucrose medium [35]. They may also contain polyalcohols, some of which, such as galactitol, manitol and sorbitol, yield high concentrations of stable polyolate complexes containing hexa-coordinated silicon [22]. The amorphous products formed (carbonates, silicates, sulfates) might be intermediate thaumasite precursors.

Temperature played an important role in the case for nitrate-based admixtures (sample 5). Thaumasite was observed after 6 months in the samples cured at 5 °C, which was not the case for the samples stored at 25 °C. The admixture appeared not to inhibit C-S-H gel precipitation at 5 °C, but it did favour the change from tetrahedral to octahedral Si.

Finally, temperature also had a significant effect on thaumasite formation in carboxylate and polysulfonate-based precipitates (retarding admixture 10), since thaumasite was only observed in sample 10B, which was cured at 5 °C. The more dilute form of the admixture interfered substantially with sulfate precipitation, although the silicates appeared to precipitate normally. Nonetheless, with time it favoured the change in Si coordination and thaumasite precipitation. According to Neville [29], retarding admixtures are believed to modify crystal growth or morphology, adsorbing onto the rapidly forming membrane of hydrated cement and retarding the growth of calcium hydroxide nuclei.

Retarding admixtures are normally used at high temperatures and their effect declines in cooler environments. This study showed that, at the lowest concentrations, thaumasite formed in the presence of retarding admixtures at low temperatures.

As a rule accelerating admixtures are used at low temperatures, since when the temperature rises the drying rate is so high that it may cause shrinkage cracking. In the present study we have demonstrated that thaumasite can be formed with accelerating admixtures at low temperatures (5 °C), while thaumasite was not formed at 25 °C.

The methodology applied in this study would have to be validated and refined, but in principle it distinguished between admixtures that did and those that did not favour thaumasite formation.

5. Conclusions

This study proposes a working methodology to differentiate between admixtures that do and do not favour thaumasite precipitation.

The findings show that some admixtures furthered thaumasite precipitation when in contact with a solution containing sodium silicates, carbonates and sulfates and CaO. This effect was more noticeable at lower temperature (5 °C).

The polycarboxylate- and thiocyanate-based products were the only admixtures studied that did not inhibit C–S–H gel, calcite and portlandite precipitation as well as did not promote thaumasite formation.

Lignosulfonates furthered thaumasite formation, particularly at low temperatures, after the initial precipitation of amorphous compounds (possibly reaction precursors).

The mixes containing sodium carboxylate and polysulfonate also favoured thaumasite formation, especially at low temperatures.

Sodium aluminate or aluminium sulfate-based admixtures also fostered precipitation of the salt, particularly at low temperatures and concentrations.

Acknowledgements

This research was funded by the Spanish Ministry of Education and Science (MAT2006-11705; C31/2006 and CONSOLIDER CSD2007-00058) and the Regional Government of Madrid (Geomaterials Programme). The authors would like to thank Sika S.A.U. for providing admixtures and Patricia Rivilla for her help in the development of experimental work.

References

- [1] Thaumasite Expert Group, Great Britain, Rotherham, DETR, London, 1999.
- [2] M.I. Sánchez de Rojas, R. Sotolongo, M. Frías, F. Marín, J. Rivera, E. Sabador, Decay of pavement mortar due to thaumasite formation, *J. Chem. Technol. Biotechnol.* 84 (3) (2009) 320–325.
- [3] P.W. Brown, A. Doerr, Chemical changes in concrete due to ingress of aggressive species, *Cem. Concr. Res.* 30 (2000) 411–418.
- [4] S. Diamond, Microscopic features of ground water induced sulphate attack in highly permeable concretes, in: V.M. Malhotra (Ed.), *Proceedings of the Fifth CANMET/ACI International Conference on Durability of Concrete*, Am. Concr. Inst. SP-192, Barcelona, Spain, 2000, pp. 403–416.
- [5] S. Sahu, S. Badger, N. Thaulow, Evidence of thaumasite formation in Southern California concrete, *Cem. Concr. Compos.* 24 (2002) 379–384.
- [6] S. Diamond, Thaumasite in Orange County, Southern California: an inquiry into the effect of low temperature, *Cem. Concr. Compos.* 25 (8) (2003) 1161–1164.
- [7] J. Bensted, Thaumasite—the route to current understanding, *Cement Wapno Gips* 4 (2007) 165–178.
- [8] P. Nobst, J. Stark, Investigations on the influence of cement type on thaumasite formation, *Cement Concr. Compos.* 25 (2003) 899–906.
- [9] D.M. Mulenga, P. Nobst, J. Stark, Thaumasite formation in concrete and mortars containing fly ash, *Cem. Concr. Compos.* 25 (2003) 907–912.
- [10] F. Bellmann, J. Stark, The role of calcium hydroxide in the formation of thaumasite, *Cem. Concr. Res.* 38 (2008) 1154–1161.
- [11] J. Aguilera, S. Martínez-Ramírez, I. Pajares-Colomo, M.T. Blanco-Varela, Formation of thaumasite in carbonated mortars, *Cem. Concr. Compos.* 25 (2003) 991–996.
- [12] F. Bellmann, W. Erfurt, H.M. Ludwig, Field performance of concrete exposed to sulphate and low pH conditions from natural and industrial sources, *Cem. Concr. Compos.* 34 (1) (2012) 86–93.
- [13] G.C. Long, Y.-J. Xie, D.-H. Deng De-hua, X.-K. Li, Deterioration of concrete in railway tunnel suffering from sulfate attack, *J. Cent. South Univ. Technol.* 18 (2011) 881–888.
- [14] X.-G. Tang, Y.-J. Xie, G.-C. Long, Deterioration of actual railway tunnel lining in southwest China: geotechnical, material & structural, in: Jiang, et al., (Eds.), *Geomechanics and Geotechnics, Micro to Macro*, Taylor & Francis Group, London, 2011, pp. 1161–1165, From.
- [15] F. Sandrone, V. Labiouse, Identification and analysis of Swiss National Road tunnels pathologies, *Tunnelling Underground Space Technol.* 26 (2011) 374–390.
- [16] M.T. Blanco-Varela, J. Aguilera, S. Martínez-Ramírez, Effect of cement C₃A content, temperature and storage medium on thaumasite formation in carbonated mortars, *Cem. Concr. Res.* 36 (2006) 707–715.
- [17] J. Bensted, Thaumasite: a deterioration product of hardened cement structures, *Il Cemento* 1 (1988) 3–10.
- [18] J. Aguilera, Efectos provocados por el ataque conjunto de los agents atmosféricos CO₂ y SO₃. Condiciones termodinámicas que permiten la formación de thaumasita y sus efectos destructivos en los morteros de cemento. PhD Thesis (2003) Universidad Autónoma de Madrid, Spain.
- [19] L.J. Struble, Synthesis and characterization of ettringite and related phases, VIII International Congress on the Chemistry of Cement, Abila Grafica e Editora Ltda, Rio de Janeiro, 1986, pp. 582–588.
- [20] J. Aguilera, M.T. Blanco-Varela, T. Vázquez, Procedure of synthesis of thaumasite, *Cem. Concr. Res.* 31 (2001) 1163–1168.
- [21] S. Martínez-Ramírez, M.T. Blanco-Varela, J. Rapazote, Thaumasite formation in sugary solutions: effect of temperature and sucrose concentration, *Constr. Build. Mater.* 25 (2011) 21–29.
- [22] S.D. Kinrade, J.W. Del Nin, A.S. Schach, T.A. Sloan, K.L. Wilson, C.T.G. Knight, Stable five- and six-coordinated silicate anions in aqueous solution, *Science* 285 (5433) (1999) 1542–1545.
- [23] D. Kulik, GEMS-PSI v.2, PSI-Villigen, Switzerland, <http://gems.web.psi.ch/2007>.
- [24] W. Hummel, U. Berner, E. Curti, F.J. Pearson, T. Thoenen, Nagra/PSI Chemical Thermodynamic Data Base 01/01, Universal Publishers/uPublish.com, Parkland, Florida, 2002.
- [25] T. Schmidt, B. Lothenbach, M. Romer, K. Scrivener, D. Rentsch, R. Figi, Thermodynamic and experimental study of the conditions of thaumasite formation, *Cem. Concr. Res.* 38 (2008) 337–349.
- [26] S.J. Barnett, D.E. Macphee, N.J. Crammond, Extent of immiscibility in the ettringite–thaumasite system, *Cem. Concr. Compos.* 25 (2003) 851–855.
- [27] R. Skapa, F.P. Glasser, The optimum sulfate content of Portland cement, 21th Fall Meeting of the NANOCCEM CONSORTIUM April 12–14, 2011, p. 56, The Industrial-Academic Research Network on Cement and Concrete, Florence, Italy.
- [28] I. Odler, Interaction between gypsum and the C–S–H phase formed in C3S hydration, *Proceedings of VII International Congress on the Cement Chemistry Paris, IV*, 1980, pp. 493–495.
- [29] A.M. Neville, *Properties of Concrete*, fourth ed. Addison-Wesley Longman Limited, Essex, 1996.
- [30] M. Collepardi, Thaumasite formation and deterioration in historic buildings, *Cem. Concr. Compos.* 21 (1999) 147–154.
- [31] S.J. Barnett, C.D. Adam, A.R.W. Jackson, Solid solutions between ettringite and thaumasite, *J. Mater. Sci.* 35 (2000) 4109–4114.
- [32] S.J. Barnett, D.E. Macphee, E.E. Lachowski, N.J. Crammond, XRD, EDX and IR analysis of solid solutions between thaumasite and ettringite, *Cem. Concr. Res.* 32 (2002) 1–12.
- [33] H. Nebel, M. Neumann, C. Mayer, M. Eppe, On the structure of amorphous calcium carbonates. A detailed study by solid-state NMR spectroscopy, *Inorg. Chem.* 47 (2008) 7874–7879.
- [34] O. Varela, Oxidative reactions and degradations on sugars and polysaccharides, *Adv. Carbohydr. Chem. Biochem.* 58 (2003) 307–369.
- [35] M.T. Blanco-Varela, F. Rubio, M.A.G. Aranda, A.G. de la Torre, S. Martínez-Ramírez, Thermal behaviour of thaumasite, 13th ICCG. Madrid, 2011, July.